Hot Electrons Produced by Resonance Absorption in a Microwave-Plasma Interaction

Ann Y. Lee, Y. Nishida,[a] N. C. Luhmann, Jr., S. P. Obenschain,[b] B. Gu, and M. Rhodes
University of California, Los Angeles, California 90024

and

J. R. Albritton
Lawrence Livermore National Laboratory, Livermore, California 94550

and

E. A. Williams
University of Rochester, Rochester, New York 14627

(Received 6 July 1981)

The enhanced electric fields and suprathermal electron production due to resonance absorption of a microwave beam in an inhomogeneous plasma are investigated. At unexpectedly low driver-field amplitudes, the enhanced field amplitude and associated electron acceleration are apparently limited by wave breaking rather than convection. In the wave-breaking regime, a simple cold-plasma model accurately predicts many of the results, including the observed increase in wave-breaking time, and decrease in hot-electron energy obtained upon use of a finite-bandwidth driver.

PACS numbers: 52.25.Lp, 52.25.Ps

Resonance absorption[1-7] and the accompanying suprathermal electron production are important in laser-plasma interactions, particularly at the longer laser wavelengths. Here we present the first detailed investigation of electromagnetic radiation (microwaves) in an inhomogeneous plasma where the interaction is dominated by resonance absorption with the field amplitude limited by wave breaking. Specifically, we have concentrated on the initial-value problem concerning growth and saturation of the waves before extensive density-profile modifications can occur. For this essentially fixed-profile case, we find that (1) there is a broad region of incident powers over which a cold-plasma wave-breaking model accurately predicts the field growth and saturation and the accompanying accelerated electron energies; (2) the wave-breaking regime occurs at much lower incident powers than expected; (3) moderate driver bandwidth reduces the maximum field amplitude and electron energies; (4) the effects of driver bandwidth including increases in wave-breaking time and reductions in field intensities and hot-electron energies are in good agreement with a cold-plasma wave-breaking model.[5]

It is helpful to review briefly the predictions of the cold-plasma wave-breaking model. A Lagrangian plasma description with $\delta_0 = eE_d/m\omega_0^2 \ll L$ yields the displacement equation

$$\ddot{\delta} + \omega_p^2(x_0)\delta = \delta_0\omega_0^2 \exp(i\omega_0 t), \tag{1}$$

where $\omega_p^2(x_0) = \omega_0^2(1 + x_0/L)$ and $x = x_0 + \delta(x_0, t)$. The driving electric field E_d is related to the vacuum field E_0 by

$$E_d = E_0\varphi(\tau)/(2\pi k_0 L)^{1/2}, \tag{2}$$

where $\tau = (k_0 L)^{1/3}\sin\theta$ with θ the angle of incidence and $\varphi(\tau)$ is the resonance function.[1] Wave breaking occurs when $\partial\delta/\partial x_0 = -1$ which yields the wave-breaking time

$$t_b = (1/\omega_0)(8L/\delta_0)^{1/2} \propto P^{-0.25}, \tag{3}$$

where P is the incident rf power. In addition, the wave-breaking electric field intensity satisfies $E_b^2 \propto P^{0.5}$. Electrons are ejected with velocity $\langle\dot{\delta}\rangle^2 \simeq 2\omega_0^2 L\delta_0$ which results in a maximum energy $\mathcal{E}_m \simeq m\omega_0^2 L\delta_0 \propto P^{0.5}$. Simulations have shown that the suprathermal temperature $T_h \propto \mathcal{E}_m$ although the thermalization mechanism is still under discussion.[6]

A finite-bandwidth pump can be treated by substituting $\exp[i\omega_0 t + i\varphi(t)]$ in Eq. (1) where $\varphi(t)$ is a random phase function with

$$\langle\exp[i\varphi(t) - i\varphi(t')]\rangle = \exp(-\Delta\omega|t - t'|). \tag{4}$$

Solving for the ensemble-averaged quantities in the limit $\Delta\omega \gg \omega_0 x/2L$ and $\Delta\omega t \gg 1$ we obtain

$$t_b/t_{b0} = 1.02[(L/\delta_0)(\Delta\omega/\omega_0)^2]^{1/6} \tag{5}$$

and

$$E_b^2/E_{b0}^2 = \mathcal{E}_m/\mathcal{E}_{m0} = [(3\delta_0/8L)(\omega_0/\Delta\omega)^2]^{1/3}. \tag{6}$$

These indicate that t_b increases with bandwidth

while E_b and $\mathcal{E}_m$ decrease with bandwidth. However, since the total energy absorption is unaffected, the hot-electron density should increase.

The experiments were performed in an unmagnetized inhomogeneous plasma (60 cm diam, 80 cm length, 50 cm gradient scale length). Linearly polarized, pulsed microwave radiation ($f_0 = \omega_0/2\pi \simeq 3$ GHz) of typical rise time $\tau_0 \simeq 2-10$ ns and $\simeq 25\times 38$ cm size is launched with $\theta \simeq 12°-14°$. The experiments were performed in the plasma afterglow which is completely Maxwellian with $n_e \simeq 10^{11}$ cm^{-3}, $n_n \simeq 10^{13}$ cm^{-3}, $T_e \simeq 1$ eV, and $T_e/T_i \simeq 5$. Electron distributions are obtained with movable, shielded, retarding-grid energy analyzers. Electric fields are determined with shielded, miniature coaxial probes. Probe measurements in the vicinity of the resonance layer may be subject to error due to local perturbations. However, we did not observe any effect on nonperturbing diagnostics located away from this region (such as energy analyzers and magnetic probes) when electric probes were moved into the critical layer. In addition, the relative electric-probe measurements were consistent with the others lending further strength to their validity. By mixing narrow-band rf with random noise, a random amplitude-modulated driver of adjustable bandwidth permitted the study of finite bandwidth control similar to earlier work on spontaneous field generation and the parametric decay instability.[8-10]

We concentrate on the initial-value problem of the growth and saturation of the phenomena with resonance absorption during the first 0.5 μs ($\omega_{pe}\tau \leq 10^4$) when the profile is essentially fixed so that the analytic theory can be expected to apply. Figure 1(a) shows the growth of the peak electric field near the critical layer. The field grows until it reaches a maximum value ($\omega_{pi}\tau \simeq 20$) after which it collapses to $\simeq$(10-15)% of its peak value. The saturation of the field appears to be consistent with wave breaking. Figure 1(b) shows the scaling of the peak field intensity E_b^2 and time t_b versus incident power. For 50 W $\leq P \leq$ 600 W ($3\times 10^{-4} < \eta_{vac} = E_0^2/8\pi KT_e \leq 4\times 10^{-3}$), the profile modifications are small (< 14%) and we find $t_b \propto P^{-0.31}$ and $E_b^2 \propto P^{0.64}$ in agreement with the predicted $P^{-0.25}$ and $P^{0.5}$ dependences. For P > 600 W, the scalings change to $t_b \propto P^{-1.2}$ and $E_b^2 \propto P^{1.47}$. However, the present discussion is restricted to the low-power region. The measured time scales are also in quantitative agreement with the wave-breaking model. Using our parameters, we estimate that $E_d \simeq 2.77$ V/cm at $P = 500$ W. This results in a predicted wave-breaking

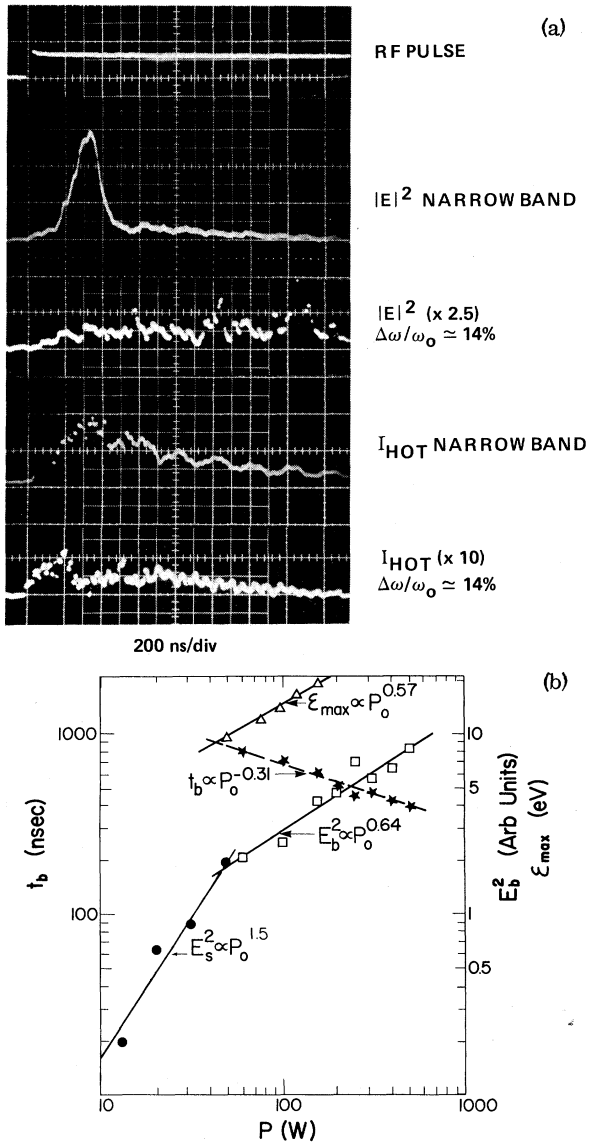

FIG. 1. (a) Time histories of rf pulse ($P = 500$ W), narrow-band critical-layer electric field intensity, finite-bandwidth ($\Delta\omega/\omega = 14\%$) field intensity, narrow-band hot-electron current (> 20 eV) and finite-bandwidth hot-electron current. (b) Scaling of narrow-band electric field intensity, maximum cutoff energy, and wave-breaking time with incident power.

time of $\simeq$ 290 ns which is in good agreement with the measured value of $\simeq$ 300-350 ns. Finally, Langmuir probe measurements of the time evolution and absolute intensities of the second and third harmonics of the electrostatic field (relative to the fundamental) were in agreement with predictions of cold-plasma theory. Coincident with the electric field growth, a burst of hot electrons is observed. The hot-electron tail distribu-

tion is found to be Maxwellian with temperature T_h up to a maximum energy $\mathcal{E}_m$ where the distribution rapidly decreases. The electron energy-analyzer current at the wave-breaking time approximately 3 cm below critical is shown in Fig. 2 as a function of analyzing voltage, both with and without rf. The formation of the energetic electron tail is clearly seen. We find that both the upper energy cutoff $\mathcal{E}_m$ and T_h scale as $P^{0.6}$ with the former in agreement with the cold-plasma model. For $P > 600$ W, a two-temperature hot-electron tail develops.

The above data show good agreement with wave-breaking theory for $50\ \text{W} < P < 600$ W. However, for these conditions, Langmuir wave convection is predicted to limit the field amplitude rather than wave breaking.[11] The calculated convective saturation time is $\simeq 75$–100 ns. Referring to Fig. 1(a) we see that there is in fact a first peak or shoulder on the $|E|^2$ trace (smaller than the wave-breaking amplitude) at $\simeq 100$–150 ns after rf turn-on. We investigated the scaling of the amplitude of this peak and find that it is $\propto P^{0.81}$, in reasonable agreement with the expected linear power scaling for convective saturation. In addition, the time at which this first peak occurs was found to be independent of power as expected for convective saturation. The continued growth (and agreement with cold-plasma wave-breaking theory) is explained by the fact that before convective saturation is reached we already have $v_{\text{wave}} = eE_{\text{wave}}/m\omega \gtrsim v_{te}$ and the thermal convection picture is suspect. To more clearly see this transition we performed detailed measurements for $0.1\ \text{W} \lesssim P \lesssim 600$ W. We find that below $P = 50$ W ($v_{\text{wave}} \simeq v_{te}$) the transition toward convective saturation begins. Specifically, for $8\ \text{W} \lesssim P_0 \lesssim 50$ W we find $E_{\text{sat}}^2 \propto P^{1.5\text{-}1.8}$ [see Fig. 1(b)]. However, not until $P_0 \lesssim 1$ W do we begin to observe "pure" convective saturation. This is considerably lower than the power level which is predicted from the commonly used estimate of $E_{\text{conv}} \simeq E_B$ for the transition.

Finite-bandwidth pump effects were studied. Figure 1(a) shows the electric field growth near the critical layer for both narrow-band and finite-bandwidth pumps. The increase in the wave-breaking time and decrease in wave-breaking field amplitude in the finite-bandwidth case is obvious. The wave-breaking time and critical-layer electric field intensity are plotted in Fig. 3 as a function of the bandwidth of a random amplitude-modulated pump (solid lines, theory). The average power was maintained at $P = 520$ W for the data shown. The agreement is seen to be excellent.

As shown in Fig. 2, finite bandwidth reduces T_h and $\mathcal{E}_m$. Detailed measurements were made of the dependence of T_h and $\mathcal{E}_m$ on pump bandwidth for an incident power of 150 W. The cutoff energy was $\mathcal{E}_m \propto (\Delta\omega/\omega_0)^{-0.67}$ in close agreement with the predicted $(\Delta\omega/\omega_0)^{-2/3}$ scaling. T_h scales very differently with bandwidth $[\propto(\Delta\omega/\omega_0)^{-0.31}]$ than

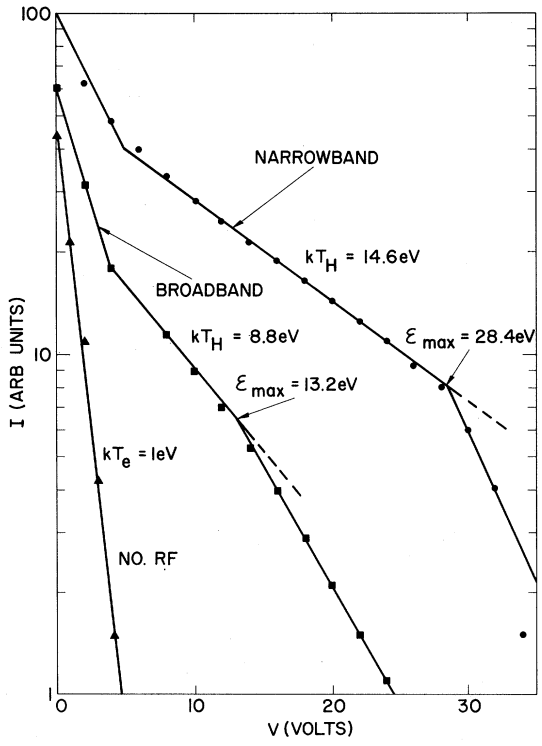

FIG. 2. Energy analyzer current vs analyzing voltage both without rf and with narrow-band and finite-bandwidth pumps ($P = 150$ W).

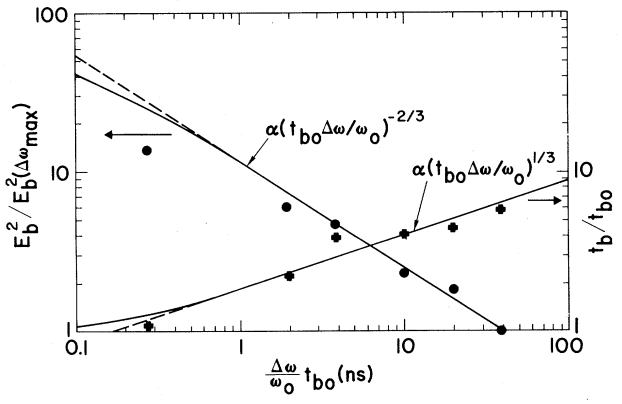

FIG. 3. Comparison of measured wave-breaking field and time dependence on pump bandwidth with cold-plasma wave-breaking theory [Eqs. (5) and (6)].

$\mathcal{E}_m$. Spielman *et al.*[12] observed a similar bandwidth effect on T_h. However, the most striking and important effect appears to be the reduction in $\mathcal{E}_m$ observed in our experiment and predicted theoretically.

The total number of hot electrons also decreases as the bandwidth is increased ($n_h \propto (\Delta\omega/\omega_0)^{-0.43}$). One would not expect finite bandwidth to affect the amount of energy deposited through resonance absorption on the basis of the cold-plasma model. However, we find experimentally considerable reductions in profile modifications (2.7% vs 14%) which could in turn change the total absorption.

In conclusion, we have shown that at low power levels the cold-plasma wave-breaking model accurately predicts the wave-breaking time t_b, scaling of the electric field E_b, and maximum wave-breaking energy $\mathcal{E}_m$. Furthermore, the hot-electron temperature T_h scales with $\mathcal{E}_m$. The transition from convective saturation to wave-breaking saturation was found to occur when $v_{wave} \simeq v_{te}$. Finally, we have shown that finite pump bandwidth reduces the hot-electron temperature, increases the wave-breaking time, and decreases the field amplitude and maximum electron energy as predicted.

This work was supported by U. S. Department of Energy Contract No. DE-AS08-81 DP40143 and by the U. S. Air Force Office of Scientific Research Contract No. F49620-76-C-0012.

[a]Permanent address: Faculty of Engineering, Utsunomiya University, Utsunomiya, Japan.
[b]Permanent address: Naval Research Laboratory, Washington, D. C. 20375.
[1]V. L. Ginsburg, *The Properties of Electromagnetic Waves in Plasmas* (Pergamon, New York, 1964).
[2]D. W. Forslund, J. M. Kindel, and K. Lee, Phys. Rev. Lett. 39, 284 (1977).
[3]K. Estabrook and W. L. Kruer, Phys. Rev. Lett. 40, 42 (1978).
[4]J. R. Albritton and A. B. Langdon, Phys. Rev. Lett. 45, 1794 (1980).
[5]E. A. Williams and J. R. Albritton, in Proceedings of the Ninth Annual Conference on Anomalous Absorption of Electromagnetic Waves, Rochester, N. Y., 15–18 May 1979 (unpublished), paper C-2.
[6]B. Bezzerides, S. J. Gitomer, and D. W. Forslund, Phys. Rev. Lett. 44, 651 (1980).
[7]P. Koch and J. Albritton, Phys. Rev. Lett. 32, 1420 (1974).
[8]S. P. Obenschain and N. C. Luhmann, Jr., Phys. Rev. Lett. 42, 311 (1979).
[9]S. P. Obenschain, N. C. Luhmann, Jr., and P. T. Greiling, Phys. Rev. Lett. 36, 1309 (1976).
[10]S. P. Obenschain and N. C. Luhmann, Jr., Appl. Phys. Lett. 30, 452 (1977).
[11]K. G. Estabrook, E. J. Valeo, and W. L. Kruer, Phys. Fluids 18, 1151 (1975).
[12]R. B. Spielman, W. M. Bollen, K. Mizuno, and J. S. DeGroot, Phys. Rev. Lett. 46, 821 (1981).

Class of Model Stellarator Fields with Enhanced Confinement

H. E. Mynick,[a] T. K. Chu, and A. H. Boozer
Princeton Plasma Physics Laboratory, Princeton University, Princeton, New Jersey 08544
(Received 6 July 1981)

A class of model stellarator fields has been found in which the transport is reduced by an order of magnitude from transport in conventional stellarators, by localizing the helical ripple to the inside of the torus. The reduction is observed in numerical experiments, and explained theoretically. Realizations of this class are achievable with use of modular coils.

PACS numbers: 52.55.Gb

We report here on the discovery of a family of model stellarator configurations having transport which is greatly reduced from that which has been theoretically predicted,[1,2] and observed in numerical experiments,[3] for the standard configuration traditionally envisioned. Such an enhancement of confinement is important, since the transport levels predicted by the theory of Refs. 1 and 2 may be too large to make a stellarator reactor of acceptable size.

The new configurations are related to one proposed by Meyer and Schmidt[4] (the MS configuration). There, the objective was to improve the equilibrium properties at high β (the ratio of the pressures of the plasma and the confining magnetic field) by reducing the Pfirsch-Schluter currents J_{PS}. This is achieved by localizing the ripple in the magnetic field $\vec{B}$ induced by the helical

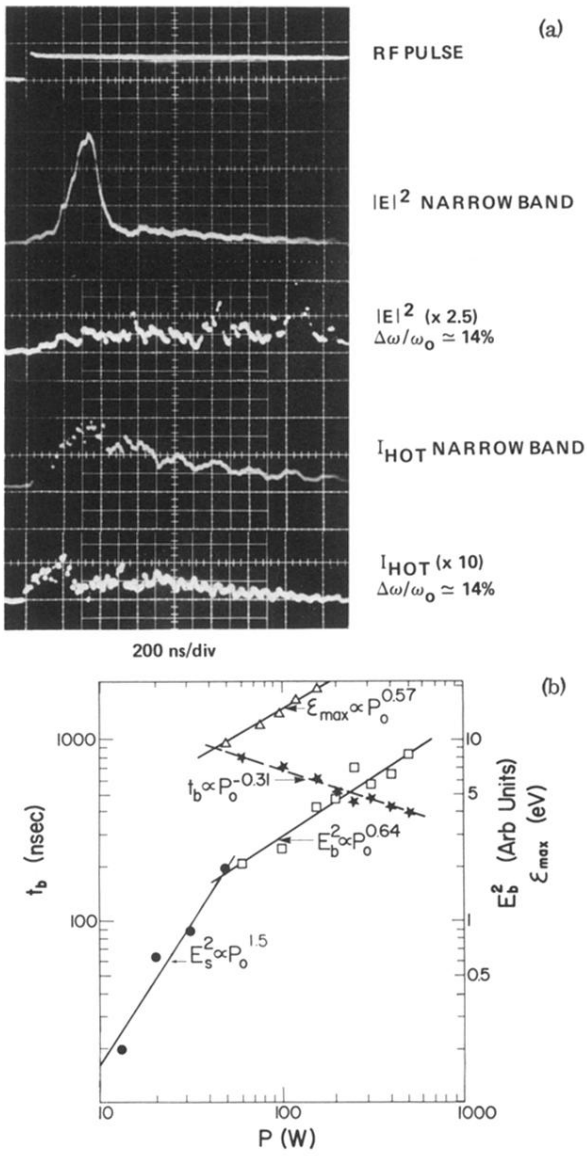

FIG. 1. (a) Time histories of rf pulse ($P = 500$ W), narrow-band critical-layer electric field intensity, finite-bandwidth ($\Delta\omega/\omega = 14\%$) field intensity, narrow-band hot-electron current (> 20 eV) and finite-bandwidth hot-electron current. (b) Scaling of narrow-band electric field intensity, maximum cutoff energy, and wave-breaking time with incident power.